

Thermomechanical Properties of Non-Stoichiometric Gadolinium Doped Ceria by Molecular Dynamics Simulations

Zhiwei Cui¹, Yi Sun^{1,*}, and Jianmin Qu²

¹Department of Astronautic Science and Mechanics, Harbin Institute of Technology Harbin, 150001, P. R. China

²Department of Mechanical Engineering, Northwestern University, Evanston, IL 60208, USA

Gadolinium doped ceria (GDC) will undergo chemical reduction reaction, yielding a discharge of the formal charged Ce^{4+} to Ce^{3+} under a low oxygen partial pressure. The effect of such chemical change on the mechanical response can be quantified by coefficient of compositional expansion (CCE) and elastic constants. In a recent paper, *ab initio* interionic pair potentials for GDC systems are derived based on the quantum mechanical calculation. Simulation results prove that the potential is reasonably good to be used for broad atomic simulations, except unphysical Cauchy relation. Consequently, in the current work, we propose an empirical three-body potential to modify the original *ab initio* interionic pair potential for GDC systems. The quality of the proposed potentials is verified by molecular dynamics simulations of CeO_2 and solid solution GDC. We then use the potential to calculate the doped concentrations and temperature dependence of CCE and elastic constants. The CCE fits well with experiment data 0.06~0.08. Meanwhile, the Young's modulus decreases with increasing vacancy concentration, while the variation of the Poisson's ratio is found to be negligible. In addition, both the elastic constants and the CCE are found to be insensitive to temperature.

Keywords: Empirical Three-Body Potential, *Ab Initio* Potential, Gadolinia-Doped Ceria, Molecular Dynamics Simulation, Elastic Constants.

1. INTRODUCTION

For the last decades, solid electrolytes have achieved amount of attentions due to their applications in solid oxide fuel cells (SOFC) or oxygen sensors. Especially, rare earth-doped ceria are widely used as the intermediate temperature electrolyte. To this end, both experiments and atomic scale simulations have been performed extensively.¹⁻³ However, the matrix ceria will swell under a low oxygen partial pressure,⁴ yielding a discharge of the uniformly charged Ce^{4+} to Ce^{3+} . Some additional oxygen vacancies are generated to keep electric neutrality. Obviously, such point defects will attenuate the mechanical performance of electrolyte.⁵

To study the evolution behavior of non-stoichiometric gadolinia-doped ceria (GDC), the molecular dynamics (MD) method is adopted in this work. MD is proved to be a powerful technique to investigate the microscopic nature of atomic motion. With MD method, many literature

work⁶⁻¹¹ have studied various properties of GDC. However, most of them are based on the empirical potential and different potential parameters may give divergent results. Recently, an *ab initio* interionic potential for GDC¹² is proposed by the current authors based on quantum physical calculations¹³⁻¹⁷ and verified by a bunch of MD simulations in various categories on CeO_2 , GDC and non-stoichiometric GDC. Simulation results prove that the potential is reasonably good to be used for broad atomic simulations. However, due to the pairwise potential, the unphysical Cauchy relation ($C_{12} = C_{44}$) is always held. Such drawback will reduce the calculation accuracy inevitably, especially in predicting the crack propagation and fracture criteria. In particular, some mechanical properties, such as coefficient of compositional expansion (CCE) and elastic constants, are needed in the continuum electrochemomechanical coupling modeling.¹⁸ Therefore, one empirical three-body interaction is introduced in this paper by fitting the mismatch between pairwise potential and experiment data. Such modification is then used

*Author to whom correspondence should be addressed.

to predict the mechanical properties of non-stoichiometric GDC system by MD simulations.

2. THREE-BODY POTENTIAL MODELING

In ionic solids, due to the predominant Coulomb energy, we assume the three-body energy is relative small. In addition, the many-body effect grows dramatically under high pressure while the interionic distance between heterogeneous atoms becomes shorter. For instance, pairwise potential of NaCl is precise enough to describe the structure properties at normal pressure and temperature, since the Cauchy relation is satisfied approximately. However, Cauchy violation becomes significant with increasing pressure, which indicates that the three-body interactions could not be neglected. Thus the three-body interaction is relative small, and reduces with increasing of interionic separation. For simplicity, we assume the short-range three-body potential Φ^{ST} can be neglect beyond the nearest neighbor (NN) distance. In other words, such potential is used to describe the complicated interactions between the NN atoms.

In the current work, we mainly focus on the mechanical properties of the matrix CeO_2 . Fitting the elastic constants is used to provide the efficient three-body potential functions since the elasticity of materials is of substantial physical interest. For three-body potential $\Phi^{\text{ST}}(r_{ij}, r_{ik}, \theta_{ijk})$, the elastic constants can be obtained by,

$$\begin{aligned} C_{11} &= \left(\frac{\partial^2 \Phi^{\text{ST}}(a)}{\partial \varepsilon_1^2} \right)_{a=a_0} \\ C_{12} &= \left(\frac{\partial^2 \Phi^{\text{ST}}(a)}{\partial \varepsilon_1 \partial \varepsilon_2} \right)_{a=a_0} \\ C_{44} &= \left(\frac{\partial^2 \Phi^{\text{ST}}(a)}{\partial \varepsilon_4^2} \right)_{a=a_0} \end{aligned} \quad (1)$$

where ε_i is the strain tensor. The three-body potential is assumed as,

$$\begin{aligned} \Phi^{\text{ST}}(r_{ij}, r_{ik}, \theta_{ijk}) &= f(r_{ij}, r_{ik})g(\theta_{ijk}) \\ &= f(r_{ij}, r_{ik})g(\cos \theta_{ijk}) \end{aligned} \quad (2)$$

where,

$$\cos \theta = \frac{\vec{r}_{ij} \cdot \vec{r}_{ik}}{r_{ij} r_{ik}} = \frac{A(\varepsilon)}{r_{ij} r_{ik}} \quad (3)$$

and

$$\begin{aligned} \vec{r}_{ij} \cdot \vec{r}_{ik} &= A(\varepsilon) = \vec{r}_{ij0} \cdot \vec{r}_{ik0} \\ &+ a_0^2 \{ 2\varepsilon_1 r_{ijx} r_{ikx} + 2\varepsilon_2 r_{ijy} r_{iky} + 2\varepsilon_3 r_{ijz} r_{ikz} \\ &+ \varepsilon_4 (r_{ijy} r_{ikz} + r_{ijz} r_{iky}) + \varepsilon_5 (r_{ijx} r_{ikz} + r_{ijz} r_{ikx}) \\ &+ \varepsilon_6 (r_{ijy} r_{ikx} + r_{ijx} r_{iky}) \} \end{aligned} \quad (4)$$

r_0 is the equilibrium interionic distance without lattice distortion. a_0 is the equilibrium lattice constant. r_{ix} , r_{iy} and r_{iz}

are the atomic coordinates. Due to the Eq. (1), the elastic constants C_{11} , C_{12} and C_{44} are derived as,

$$\begin{aligned} C_{11} &= \frac{\partial^2 \Phi^{\text{ST}}}{\partial \varepsilon_1^2} = a_0^4 \times \left(\left(\left(\frac{\partial^2 f}{\partial r_{ij}^2} \right) \left(\frac{r_{ijx}^4}{r_{ij}^2} \right) \right. \right. \\ &+ 2 \left(\frac{\partial^2 f}{\partial r_{ij} \partial r_{ik}} \right) \left(\frac{r_{ijx}^2 r_{ikx}^2}{r_{ij} r_{ik}} \right) + \left. \left(\frac{\partial^2 f}{\partial r_{ik}^2} \right) \left(\frac{r_{ikx}^4}{r_{ik}^2} \right) \right) g \\ &+ \left(\left(\frac{\partial f}{\partial r_{ij}} \right) \left(-\frac{r_{ijx}^4}{r_{ij}^3} \right) + \left(\frac{\partial f}{\partial r_{ik}} \right) \left(-\frac{r_{ikx}^4}{r_{ik}^3} \right) \right) g \\ &+ 2 \left(\left(\frac{\partial f}{\partial r_{ij}} \right) \left(\frac{r_{ijx}^2}{r_{ij}} \right) + \left(\frac{\partial f}{\partial r_{ik}} \right) \left(\frac{r_{ikx}^2}{r_{ik}} \right) \right) \\ &\times \left(\frac{2r_{ijx} r_{ikx}}{r_{ij} r_{ik}} - \left(\frac{r_{ijx}^2}{r_{ij}^2} + \frac{r_{ikx}^2}{r_{ik}^2} \right) \cos \theta \right) \frac{\partial g}{\partial \cos \theta} \\ &+ f \left(\left(3 \frac{r_{ijx}^4}{r_{ij}^4} + 2 \frac{r_{ijx}^2 r_{ikx}^2}{r_{ij}^2 r_{ik}^2} + 3 \frac{r_{ikx}^4}{r_{ik}^4} \right) \cos \theta \right. \\ &- \left. \left(\frac{r_{ijx}^2}{r_{ij}^2} + \frac{r_{ikx}^2}{r_{ik}^2} \right) \frac{4r_{ijx} r_{ikx}}{r_{ij} r_{ik}} \right) \frac{\partial g}{\partial \cos \theta} \\ &+ f \left(\frac{2r_{ijx} r_{ikx}}{r_{ij} r_{ik}} - \left(\frac{r_{ijx}^2}{r_{ij}^2} + \frac{r_{ikx}^2}{r_{ik}^2} \right) \cos \theta \right)^2 \frac{\partial^2 g}{\partial \cos^2 \theta} \end{aligned} \quad (5)$$

Delivered by Publishing Technology to: University of Southern California
166.111.120.71 On: Wed, 12 Jun 2013 06:21:50
Copyright American Scientific Publishers

$$\begin{aligned} C_{12} &= \frac{\partial^2 \Phi^{\text{ST}}}{\partial \varepsilon_1 \partial \varepsilon_2} \\ &= a_0^4 \times \left(\left(\left(\frac{\partial^2 f}{\partial r_{ij}^2} \right) \left(\frac{r_{ijx}^2 r_{ijy}^2}{r_{ij}^2} \right) + \left(\frac{\partial^2 f}{\partial r_{ik}^2} \right) \left(\frac{r_{ikx}^2 r_{iky}^2}{r_{ik}^2} \right) \right) g \right. \\ &+ \left(\frac{\partial^2 f}{\partial r_{ij} \partial r_{ik}} \right) \left(\frac{r_{ijx}^2 r_{iky}^2 + r_{ijy}^2 r_{ikx}^2}{r_{ij} r_{ik}} \right) g \\ &+ \left(\left(\frac{\partial f}{\partial r_{ij}} \right) \left(-\frac{r_{ijx}^2 r_{ijy}^2}{r_{ij}^3} \right) + \left(\frac{\partial f}{\partial r_{ik}} \right) \left(-\frac{r_{ikx}^2 r_{iky}^2}{r_{ik}^3} \right) \right) g \\ &+ \left(\left(\frac{\partial f}{\partial r_{ij}} \right) \left(\frac{r_{ijx}^2}{r_{ij}} \right) + \left(\frac{\partial f}{\partial r_{ik}} \right) \left(\frac{r_{ikx}^2}{r_{ik}} \right) \right) \\ &\times \left(\frac{2r_{ijy} r_{iky}}{r_{ij} r_{ik}} - \left(\frac{r_{ijy}^2}{r_{ij}^2} + \frac{r_{iky}^2}{r_{ik}^2} \right) \cos \theta \right) \frac{\partial g}{\partial \cos \theta} \\ &+ \left(\left(\frac{\partial f}{\partial r_{ij}} \right) \left(\frac{r_{ijy}^2}{r_{ij}} \right) + \left(\frac{\partial f}{\partial r_{ik}} \right) \left(\frac{r_{iky}^2}{r_{ik}} \right) \right) \\ &\times \left(\frac{2r_{ijx} r_{ikx}}{r_{ij} r_{ik}} - \left(\frac{r_{ijx}^2}{r_{ij}^2} + \frac{r_{ikx}^2}{r_{ik}^2} \right) \cos \theta \right) \frac{\partial g}{\partial \cos \theta} \\ &+ f \left(\left(3 \frac{r_{ijx}^2 r_{ijy}^2}{r_{ij}^4} + \frac{r_{ijx}^2 r_{iky}^2 + r_{ijy}^2 r_{ikx}^2}{r_{ij}^2 r_{ik}^2} + 3 \frac{r_{ikx}^2 r_{iky}^2}{r_{ik}^4} \right) \cos \theta \right) \frac{\partial g}{\partial \cos \theta} \\ &+ f \left(-\left(\frac{r_{ijx}^2}{r_{ij}^2} + \frac{r_{iky}^2}{r_{ik}^2} \right) \frac{2r_{ijx} r_{ikx}}{r_{ij} r_{ik}} - \left(\frac{r_{ijx}^2}{r_{ij}^2} + \frac{r_{ikx}^2}{r_{ik}^2} \right) \frac{2r_{ijy} r_{iky}}{r_{ij} r_{ik}} \right) \frac{\partial g}{\partial \cos \theta} \end{aligned}$$

$$+f\left(\frac{2r_{ijx}r_{ikx}}{r_{ij}r_{ik}}-\left(\frac{r_{ijx}^2}{r_{ij}^2}+\frac{r_{ikx}^2}{r_{ik}^2}\right)\cos\theta\right) \\ \times\left(\frac{2r_{ijy}r_{iky}}{r_{ij}r_{ik}}-\left(\frac{r_{ijy}^2}{r_{ij}^2}+\frac{r_{iky}^2}{r_{ik}^2}\right)\cos\theta\right)\frac{\partial^2g}{\partial\cos^2\theta} \quad (6)$$

$$C_{44}=\frac{\partial^2\Phi^{\text{ST}}}{\partial\varepsilon_4^2} \\ =a_0^4\times\left(\left(\frac{\partial^2f}{\partial r_{ij}^2}\right)\left(\frac{r_{ijy}^2r_{ijz}^2}{r_{ij}^2}\right)+2\left(\frac{\partial^2f}{\partial r_{ij}\partial r_{ik}}\right)\left(\frac{r_{ijy}r_{ijz}r_{iky}r_{ikz}}{r_{ij}r_{ik}}\right)\right. \\ \left.+\left(\frac{\partial^2f}{\partial r_{ik}^2}\right)\left(\frac{r_{iky}^2r_{ikz}^2}{r_{ik}^2}\right)\right)g+\left(\left(\frac{\partial f}{\partial r_{ij}}\right)\left(-\frac{r_{ijy}^2r_{ijz}^2}{r_{ij}^3}\right)\right. \\ \left.+\left(\frac{\partial f}{\partial r_{ik}}\right)\left(-\frac{r_{iky}^2r_{ikz}^2}{r_{ik}^3}\right)\right)g+2\left(\left(\frac{\partial f}{\partial r_{ij}}\right)\left(\frac{r_{ijy}r_{ijz}}{r_{ij}}\right)\right. \\ \left.+\left(\frac{\partial f}{\partial r_{ik}}\right)\left(\frac{r_{iky}r_{ikz}}{r_{ik}}\right)\right)\times\left(\left(\frac{r_{ijy}r_{ikz}+r_{ijz}r_{iky}}{r_{ij}r_{ik}}\right)\right. \\ \left.-\left(\frac{r_{ijy}r_{ijz}}{r_{ij}^2}+\frac{r_{iky}r_{ikz}}{r_{ik}^2}\right)\cos\theta\right)\frac{\partial g}{\partial\cos\theta} \\ +f\left(\left(3\frac{r_{ijy}^2r_{ijz}^2}{r_{ij}^4}+2\frac{r_{ijy}r_{ijz}r_{iky}r_{ikz}}{r_{ij}^2r_{ik}^2}+3\frac{r_{iky}^2r_{ikz}^2}{r_{ik}^4}\right)\cos\theta\right)\frac{\partial g}{\partial\cos\theta} \\ +f\left(-2\left(\frac{r_{ijy}r_{ijz}}{r_{ij}^2}+\frac{r_{iky}r_{ikz}}{r_{ik}^2}\right)\left(\frac{r_{ijy}r_{ikz}+r_{ijz}r_{iky}}{r_{ij}r_{ik}}\right)\right)\frac{\partial g}{\partial\cos\theta} \\ +f\left(\left(\frac{r_{ijy}r_{ikz}+r_{ijz}r_{iky}}{r_{ij}r_{ik}}\right)\right. \\ \left.-\left(\frac{r_{ijy}r_{ijz}}{r_{ij}^2}+\frac{r_{iky}r_{ikz}}{r_{ik}^2}\right)\cos\theta\right)^2\frac{\partial^2g}{\partial\cos^2\theta} \quad (7)$$

According to those formulae, the three-body potential can be evaluated by fitting the elastic constants between pairwise interaction and experimental data. The three-body function Φ^{ST} is assumed as $\Phi^{\text{ST}}(r_{ij}, r_{ik}, \theta_{ijk}) = f(r_{ij})f(r_{ik})g(\theta_{ijk})$. Due to the fluorite structure characteristic of CeO_2 , the elastic constants of Φ^{ST} are:

- (1) $C_{11(\text{O})} = C_{12(\text{O})}$ and $C_{11(\text{Ce})} = C_{12(\text{Ce})}$ with $g(\theta) = 1$;
- (2) $C_{11(\text{O})} = C_{12(\text{O})} = C_{11(\text{Ce})} = C_{12(\text{Ce})}$ in the case of $g(\theta) = \cos\theta$;
- (3) $C_{11} = -2C_{12}$ with $g(\theta) = \cos^2\theta + \cos^3\theta$.

The subscript of elastic constants (O) and (Ce) are derive from three-body potential $\Phi_{\text{Ce-O-Ce}}^{\text{ST}}$ and $\Phi_{\text{O-Ce-O}}^{\text{ST}}$, respectively. Clearly, we can obtain the $C_{11}:C_{12} = 1:1$ with strategies 1 and 2. And combining with strategy 3, elastic constants C_{11} and C_{12} can be updated with objective values. Besides, we can modify the elastic constant C_{44} via

Table II. Static properties of CeO_2 under 0 K and 0 Pa.

	Lattice constant a_0 (Å)	Lattice energy E_{latt} (eV)	Bulk modulus B_0 (GPa)	Elastic constants (GPa)		
				C_{11}	C_{12}	C_{44}
Pair potential	5.418	34.30	223.1	458.2	105.6	106.1
This work (0 K)	5.399	34.22	211.2	418.9	107.3	63.8
Gotte ⁹	5.411	33.95	203.5	402	104	61
Vyas ⁷	5.411	35.21	267.9	554.2	1246	123.6
Butler ⁶	5.411	35.22	263.6	504.4	143.1	16.1
CASTEP	5.465		174.8	330.2	97.1	46.4
Expt ²⁶	5.411		236.0	403	105	60
This work (300 K)	5.410		206.87	411.4	104.6	61.1

strategy 2 since the C_{11} and C_{12} are identical. Base on the analysis above, the three-body interaction is

$$\Phi^{\text{ST}} = \lambda_1 \exp\left[\gamma_1\left(1-\frac{r_{ij}}{\eta}\right)\right] \exp\left[\gamma_1\left(1-\frac{r_{ik}}{\eta}\right)\right] \\ + \lambda_2 \exp\left[\gamma_2\left(1-\frac{r_{ij}}{\eta}\right)\right] \exp\left[\gamma_2\left(1-\frac{r_{ik}}{\eta}\right)\right] (2\cos\theta + \cos^2\theta) \\ + \lambda_3 \exp\left[\gamma_3\left(1-\frac{r_{ij}}{\eta}\right)\right] \exp\left[\gamma_3\left(1-\frac{r_{ik}}{\eta}\right)\right] \\ + \lambda_4 \exp\left[\gamma_4\left(1-\frac{r_{ij}}{\eta}\right)\right] \exp\left[\gamma_4\left(1-\frac{r_{ik}}{\eta}\right)\right] \cos\theta \quad (8)$$

The first three terms are used to modify the C_{11} , C_{12} and lattice constant of CeO_2 , while the last term is responsible for the correction of C_{44} . All the parameters of $\Phi_{\text{Ce-O-Ce}}^{\text{ST}}$ are listed in Table I. For $\Phi_{\text{O-Ce-O}}^{\text{ST}}$, we only change the $\lambda_{4(\text{O})}$ as $-\lambda_{4(\text{Ce})}$.

3. VALIDITY OF INTERIONIC POTENTIALS

We first calculate the static properties of equilibrium CeO_2 . Lattice constants, lattice energy, and elastic properties have also been calculated based on the CASTEP calculation and other empirical functions. The results are given in Table II. Clearly, such correction can improve the mechanical properties significantly.

To better assess the developed potential, we now extend the system pressure from zero to a finite wide range. The results are depicted in Figures 1 and 2. Considering the limitation of the experiments, we take CASTEP calculations as the reference. In the pressure range from 0 to 200 GPa, the lattice constants and elastic constants (Fig. 1) of our calculations and CASTEP share the same trend,

Table I. The parameters of the short-range three-body potential for CeO_2 .

λ (eV)				γ				η (Å)
λ_1	λ_2	λ_3	λ_4	γ_1	γ_2	γ_3	γ_4	
-0.04883	-0.27344	0.00021	-0.26160	4.7145	3.7663	14.667	4.9399	2.343

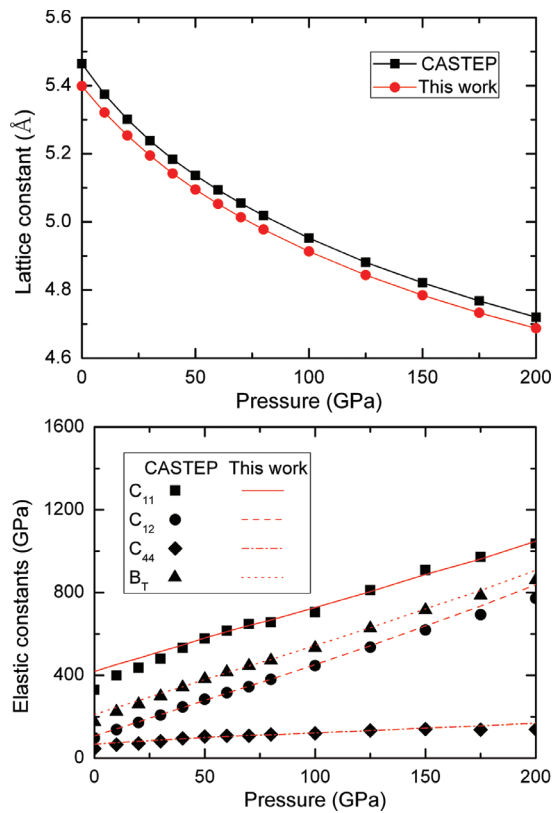


Fig. 1. Pressure dependence of the lattice constant and elastic constants from 0 to 200 GPa.

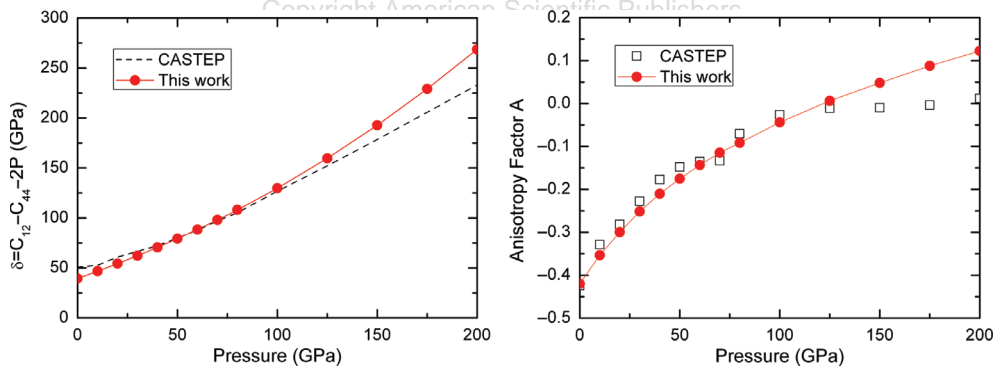


Fig. 2. Pressure dependence of the Cauchy violation and anisotropy factor from 0 to 200 GPa.

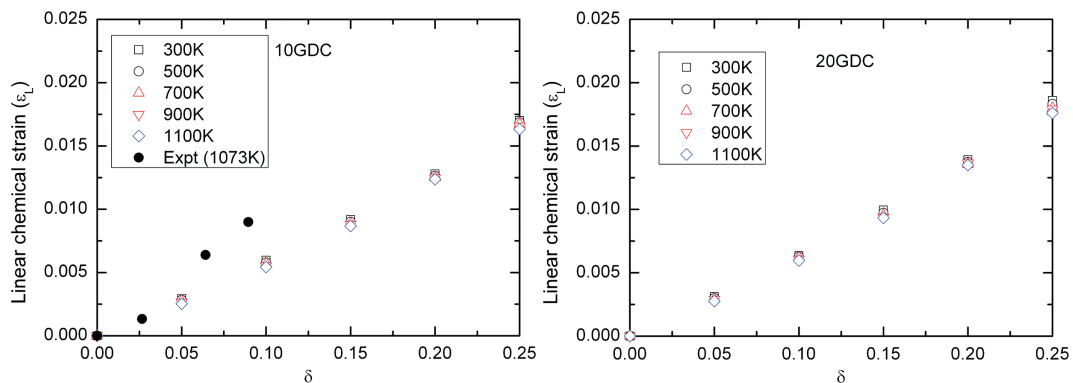


Fig. 3. Compositional strain versus δ of 10 GDC and 20 GDC.

Table III. Average CCE values of 10 GDC and 20 GDC at various temperatures.

Temperature (K)	CCE	
	10 GDC	20 GDC
300	0.06730	0.07372
500	0.06685	0.07275
700	0.06635	0.07157
900	0.06599	0.07107
1100	0.06538	0.07061

with the CASTEP ones slightly larger than ours. This is due to a larger lattice constant by CASTEP calculation at zero temperature and pressure than that from experiment. Also, note that the lattice constant reduces gradually from 5.4 Å to 4.7 Å from 0 to 200 GPa. This reveals that our interionic potential could describe the evolution of materials behaviors in extended phase space.

Figure 2 shows the pressure dependence of the Cauchy violation, which measures the contribution from the many-body interaction, since the Cauchy relation $C_{12} = C_{44} + 2P$ should be satisfied when the interionic potentials are purely central. Clearly, such the deviation for the current work becomes larger as the pressure increase, which indicates that the many-body force becomes more and more important at high pressure. In addition, the anisotropy factor shows the same tendency with CASTEP calculations (Fig. 2).

Delivered by Publishing Technology to University of Southern California
 IP: 166.111.120.71 On: Wed, 12 Jun 2013 06:21:50
 Copyright American Scientific Publishers

4. CCE OF NON-STOICHIOMETRIC GDC

In this section, we discuss the coefficient of compositional expansion (CCE) of non-stoichiometric GDC at finite temperature. The NPT ensemble is adopted, implemented by Nose-Poincare thermostat,¹⁹ metric-tensor pressostat,²⁰ and generalized leap-frog algorithm²¹ for the time integration. Wolf algorithm²² is used to estimate the Coulomb interaction. The cutoff distance is set as 10.82 Å. Each simulation is equilibrated for 1×10^6 steps. And an additional 2×10^6 steps are evolved for data collection.

The non-stoichiometric GDC is generated by forming extra vacancies besides the original ones introduced

by dopant Gd^{3+} ions. The additional vacancy concentration can be created in stoichiometric GDC when it is exposed to a low partial pressure of oxygen. The defect generates Ce^{3+} instead of Ce^{4+} and proportional oxygen vacancies. This indicates that the total number of ions decreases.

Here, we calculate the properties of 10 GDC ($\text{Ce}_{0.9}\text{Gd}_{0.1}\text{O}_{1.95}$) and 20 GDC ($\text{Ce}_{0.8}\text{Gd}_{0.2}\text{O}_{1.9}$), where gadolinium atoms replace 10% and 20% of the cerium sites in ceria, respectively. Their corresponding non-stoichiometric forms are $\text{Ce}_{0.9}\text{Gd}_{0.1}\text{O}_{1.95-\delta}$ and $\text{Ce}_{0.8}\text{Gd}_{0.2}\text{O}_{1.9-\delta}$, where the subscript δ marks the additional oxygen vacancy concentration.

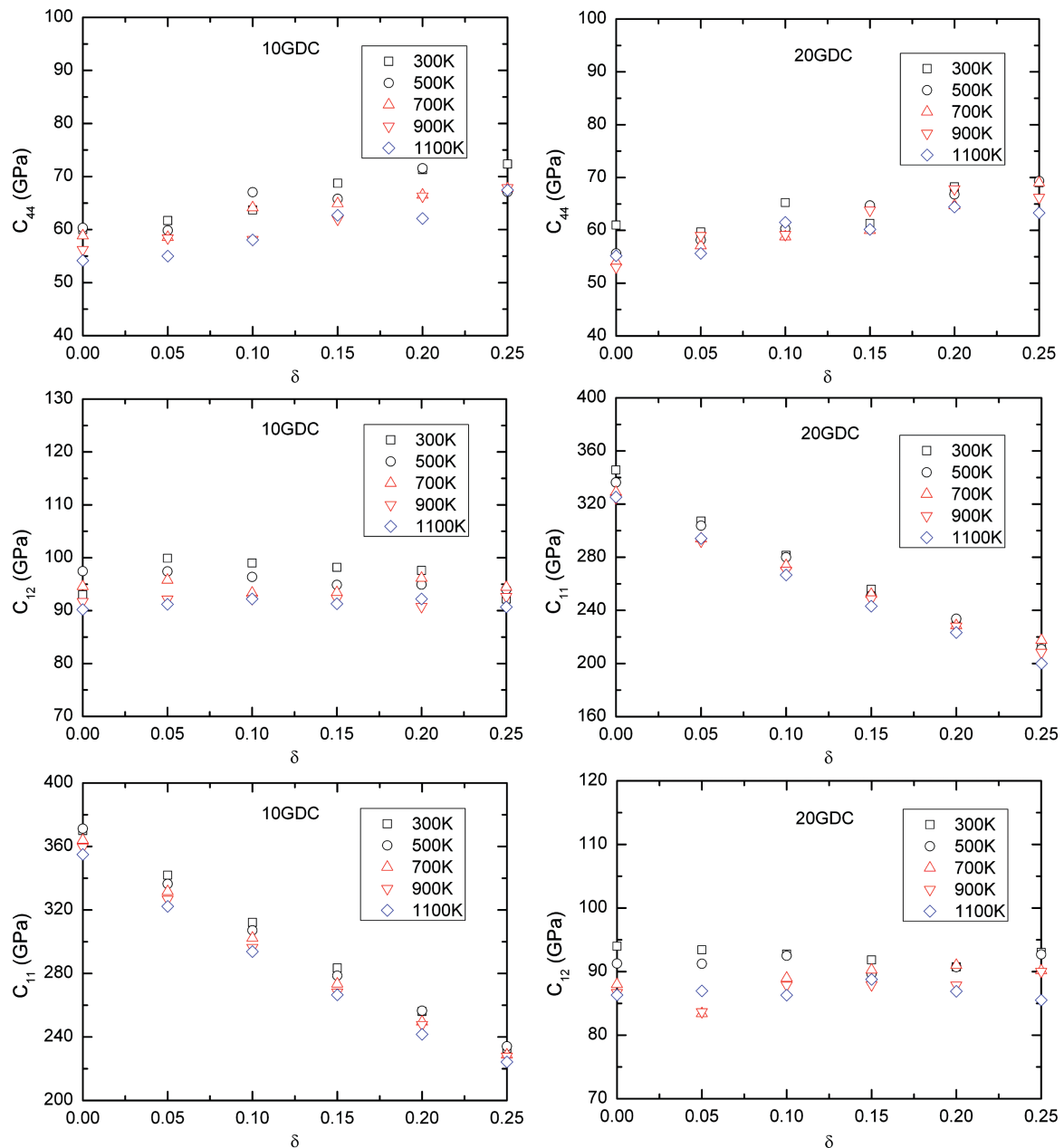


Fig. 4. Elastic constants versus δ of 10 GDC and 20 GDC.

When δ is small, CCE, denoted by η , is defined as the linear strain per deviation from stoichiometry, i.e.,

$$\eta = \left. \frac{\partial \varepsilon_L}{\partial \rho} \right|_{\rho=\rho_0} \quad (9)$$

where, ε_L is the linear chemical expansion, ρ is the vacancy concentration. $\delta = \rho - \rho_0$ is the deviation from stoichiometry. After the structure optimization, the shape of system basically remains cubic, i.e., the strain induced as a result of non-stoichiometry is purely volumetric. Thus the linear strain can be evaluated as

$$\varepsilon_L = \frac{V(\delta) - V(0)}{3V(0)} \quad (10)$$

Figure 3 depicts the relation ε_L versus δ . The results fit well with experiment data 0.06~0.08.⁴ Moreover, ε_L is proportional to the δ , leading to $\eta = \varepsilon_L/\delta$. The values of CCE for 10 GDC and 20 GDC are given in Table III.

5. ELASTIC CONSTANTS OF NON-STOICHIOMETRIC GDC

Non-stoichiometric GDC has a cubic structure, hence it has three independent elastic constants C_{11} , C_{12} and C_{44} .

These constants can be calculated directly with the stress-strain fluctuation formula.²³ Results for 10 GDC and 20 GDC are shown in Figure 4. Note that for both GDCs, C_{11} decreases rapidly with increasing δ . This is due to the weaker Coulomb interaction with larger deviation from stoichiometry. In addition, the elastic constants of 10 GDC are larger than the correspondent ones of 20 GDC. It is the consequence of lower oxygen vacancy concentration in the former case. The δ dependence of C_{12} and C_{44} is small and can be safely neglected.

Besides the properties of single crystals, the elastic constants of isotropic polycrystalline GDC should be calculated for its applications in SOFC.¹⁸ The polycrystalline properties are obtained by using a homogenization method.²⁴ Two familiar engineering properties, the Young's modulus and Poisson's ratio, are introduced instead of the elastic constants. Calculation results and experiment data²⁵ have been presented in Figures 5 and 6. Obviously, our results are smaller than the experimental measurements. Such divergence is due to smaller elastic constants by other experiment²⁶ for pure CeO_2 . Young's modulus decreases linearly with increasing deviation of stoichiometry and can be expressed as follows,

$$E = E_V^0(1 + \eta_{EV}\delta) \quad (11)$$

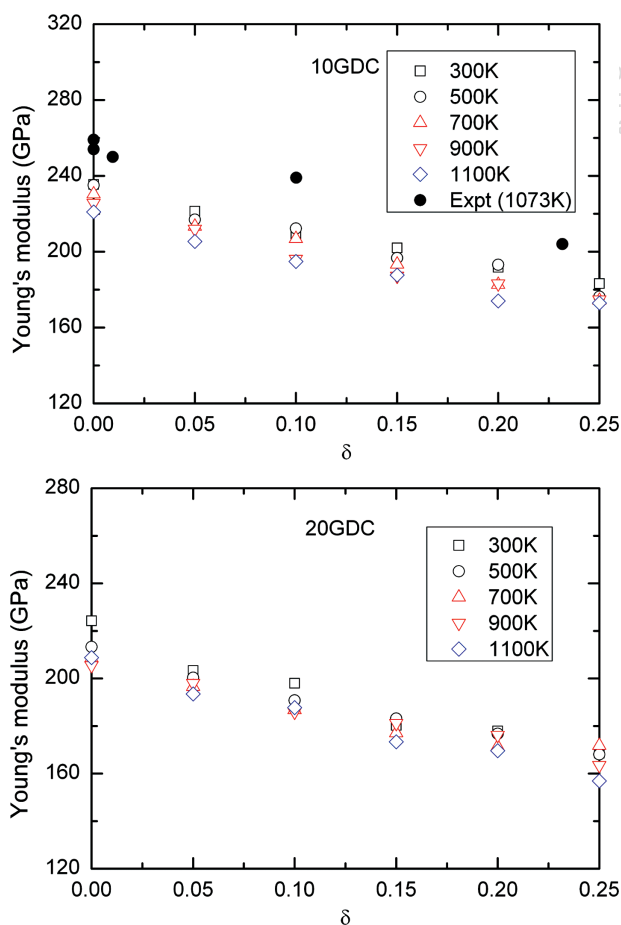


Fig. 5. Young modulus versus δ of 10 GDC and 20 GDC.

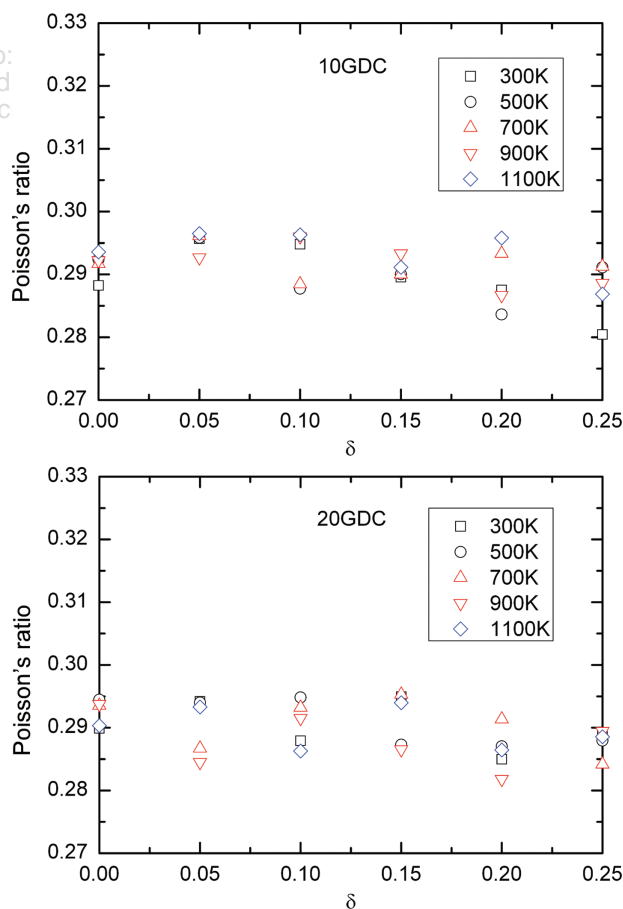


Fig. 6. Poisson's ratio versus δ of 10 GDC and 20 GDC.

Table IV. E_V^0 and η_{EV} of 10 GDC and 20 GDC at various temperature.

Temperature (K)	10 GDC		20 GDC	
	E_V^0	η_{EV}	E_V^0	η_{EV}
300	232.752	-0.87834	218.684	-0.87362
500	229.263	-0.90661	215.486	-0.90648
700	225.746	-0.93848	211.586	-0.92169
900	221.467	-0.96364	207.039	-0.94009
1100	217.037	-0.99948	203.328	-0.95713

Table IV shows the parameters E_V^0 and η_{EV} at some finite temperatures, which can be used as the input in the continuum modeling.¹⁸ Clearly, these two parameters reduce gradually with increasing temperature. Furthermore, it is found that Poisson's ratio is about 0.29 and varies within 6% over the whole range of temperature and non-stoichiometry considered here.

6. CONCLUDING REMARKS

In this paper, we propose an empirical three-body interaction of CeO₂ based on the mismatch of mechanical properties. Combining the *ab initio* pairwise potential, the newly developed potentials can predict the mechanical properties of non-stoichiometric GDC more accurately. Simulation results are consistent with corresponding experimental measurement.

In closing we point out that the three-body potential adopted here is to improve the mechanical properties of GDC. Other forms may lead to better results if a better three-body interaction potential is developed. Therefore, these new interionic potentials may be promising in exploring and predicting the properties of ionic crystals and this new method is worth further refinement and extending to other ionic crystals.

Acknowledgments: This work was supported by National Natural Science Foundation of China (10972066)

and the Foundation of Excellent Youth of Heilongjiang Province.

References

1. H. Yahiro, K. Eguchi, and H. Arai, *Solid State Ionics* 36, 71 (1989).
2. K. Eguchi, T. Setoguchi, T. Inoue, and H. Arai, *Solid State Ionics* 52, 165 (1992).
3. H. Inaba and H. Tagawa, *Solid State Ionics* 83, 1 (1996).
4. A. Atkinson, *Solid State Ionics* 95, 249 (1997).
5. K. L. Duncan, Y. L. Wang, S. R. Bishop, F. Ebrahimi, and E. D. Wachsman, *J. Am. Ceram. Soc.* 89, 3162 (2006).
6. V. Butler, C. Catlow, B. Fender, and J. Harding, *Solid State Ionics* 8, 109 (1983).
7. S. Vyas, R. W. Grimes, D. H. Gay, and A. L. Rohl, *J. Chem. Soc., Faraday Trans.* 94, 427 (1998).
8. H. Inaba, R. Sagawa, H. Hayashi, and K. Kawamura, *Solid State Ionics* 122, 95 (1999).
9. A. Gotte, D. Spangberg, K. Hermansson, and M. Baudin, *Solid State Ionics* 178, 1421 (2007).
10. X. Wei, W. Pan, L. F. Cheng, and B. Li, *Solid State Ionics* 180, 13 (2009).
11. M. Mogensen, N. M. Sammes, and G. A. Tompsett, *Solid State Ionics* 129, 63 (2000).
12. Z. Cui, Y. Sun, Y. Chen, and J. Qu, *Solid State Ionics* 187, 8 (2011).
13. S. Zhang and N. X. Chen, *Phys. Rev. B* 66, 64106 (2002).
14. S. Zhang and N. X. Chen, *J. Chem. Phys.* 118, 3974 (2003).
15. C. Wang, S. Zhang, and N. X. Chen, *J. Alloy Compd.* 388, 195 (2005).
16. H. Ohta and S. Hamaguchi, *J. Chem. Phys.* 115, 6679 (2001).
17. H. Ohta, A. Iwakawa, K. Eriguchi, and K. Ono, *J. Appl. Phys.* 104, 73302 (2008).
18. N. Swaminathan, J. Qu, and Y. Sun, *Philos. Mag.* 87, 1705 (2007).
19. S. D. Bond, B. J. Leimkuhler, and B. B. Laird, *J. Comput. Phys.* 151, 114 (1999).
20. I. Souza and J. L. Martins, *Phys. Rev. B* 55, 8733 (1997).
21. G. Sun, *J. Comput. Math.* 3, 250 (1993).
22. D. Wolf, P. Keblinski, S. R. Phillpot, and J. Eggebrecht, *J. Chem. Phys.* 110, 8254 (1999).
23. Z. Cui, Y. Sun, J. Li, and J. Qu, *Phys. Rev. B* 75, 214101 (2007).
24. B. B. Karki, L. Stixrude, S. J. Clark, M. C. Warren, G. J. Ackland, and J. Crain, *Am. Mineral.* 82, 51 (1997).
25. Y. L. Wang, K. Duncan, E. D. Wachsman, and F. Ebrahimi, *Solid State Ionics* 178, 53 (2007).
26. A. Nakajima, A. Yoshihara, and M. Ishigame, *Phys. Rev. B* 50, 13297 (1994).

Received: 19 April 2012. Accepted: 19 May 2012.